Characterization of a "Solid-State" Microelectrochemical Diode Employing a Poly(vinyl alcohol)/Phosphoric Acid Solid-State Electrolyte: Rectification at Junctions between WO_3 and Polyaniline

Nicholas Leventis, Martin O. Schloh, Michael J. Natan, James J. Hickman, and Mark S. Wrighton*

Department of Chemistry, Massachusetts Institute of Technology, Cambridge, Massachusetts 02139

Received January 26, 1990

The functionalization of an array of eight, closely spaced (~1.2 μm) Pt or Au microelectrodes each ~50 μm long, 2 μm wide, and 0.1 μm thick with redox-active WO_3 and polyaniline and the electrochemical characterization of the WO_3/polyaniline junction are reported. Chips consisting of microfabricated WO_3 covering three of the available eight microelectrodes have been analyzed by Auger electron spectroscopy. The remaining five microelectrodes are available for further derivatization with polyaniline or can function as counterelectrodes. By placing a counterelectrode and a Ag quasi-reference electrode directly on the microchip and by coating the assembly with a thin film of poly(vinyl alcohol)/H_3PO_4 solid polymeric electrolyte, the electrochemical system becomes self-contained. The solid polymer electrolyte is a good room-temperature H^+ conductor only when exposed to a H_2O-containing atmosphere. Complex impedance studies show as much as a 10^3 change in H^+ conductivity from H_2O-saturated to H_2O-free gaseous atmosphere above the polymer electrolyte. The changes in conductivity of WO_3 upon reduction or polyaniline upon oxidation allow demonstration of solid-state microelectrochemical transistors with these materials. The combination of WO_3 and polyaniline on the chip allows demonstration of a microelectrochemical diode.

We wish to report the preparation and characterization of a "solid-state" microelectrochemical diode based on the contact of microlithographically patterned WO_3 and electrochemically polymerized polyaniline on arrays of closely spaced (~1.2 μm) microelectrodes. The chip is subsequently covered with a thin film (~20 μm) of poly(vinyl alcohol)/H_3PO_4 solid-state electrolyte. Poly(vinyl alcohol)/H_3PO_4, a H_2O-swollen proton-conducting polymer blend of poly(vinyl alcohol) and H_3PO_4, has recently been proposed as the electrolyte in connection with a H_2-sensing device.[1] The polymer blend is deemed an interesting solid-state electrolyte for room-temperature applications,[1] because of its high ionic conductivity.

Murray and co-workers pioneered[2] the preparation and characterization of redox polymer bilayers to demonstrate electrochemical diodes. Our studies of WO_3 and polyaniline provide an example of such a system where both of the redox layers could become good electronic conductors upon forward bias of a diode assembly. Accordingly, the current passing through the diode may be qualitatively larger than that for electrochemical diodes based on conventional redox polymers such as the diode from poly(vinylferrocene)/polyviologen previously reported.[3]

Microelectrode arrays consisting of eight individually addressable Pt or Au microelectrodes, each ~50 μm long, ~2.2 μm wide, ~0.1 μm thick, have previously been used in our laboratory for the study of redox-active polymers and inorganic materials.[4] By taking advantage of solid-state electrolytes based on poly(ethylene oxide) (PEO),[5] poly(vinyl alcohol) (PVA),[6] and poly[bis(2-(2-methoxyethoxy)ethoxy)phosphazene] (MEEP),[7] we have demonstrated microelectrochemical systems where all ancillary components of the system (counterelectrode and reference electrode) are confined onto the chip. We have previously found[6] that the electrochemical switching properties of polyaniline using poly(vinyl alcohol)/H_3PO_4 electrolyte are essentially the same as in liquid electrolytes, except the switching speed is lower. In this report we wish to detail the electrochemical response of WO_3 using the poly(vinyl alcohol)/H_3PO_4 electrolyte medium and show that polyaniline and WO_3 can be exploited together to yield novel electrochemical systems.

Three of the five microelectrochemical systems characterized in this paper are shown in Scheme I. The thrust of our experiments is to thoroughly characterize the WO_3 and polyaniline microelectrochemical systems shown in Scheme I. These individual systems, Scheme IA,B, are referred to as microelectrochemical transistors. The characterization is key to understanding how WO_3 and polyaniline can be used together to produce other electrical functions such as the self-referencing transistors, Scheme IC, and diodelike behavior, Scheme II. By "self-referencing" in Scheme IC we mean that one redox material is used as a reference for the other such that an applied potential change, $V_G^1 \rightarrow V_G^2$, will result in simultaneous switching of both transistors.

* Address correspondence to this author.

(1) (a) Polak, A. J.; Petty-Weeks, S.; Beuhler, A. *J. Sensors Actuators* **1986**, *9*, 1. (b) Petty-weeks, S.; Polak, A. *J. Sensors Actuators* **1987**, *11*, 377. (c) Petty-Weeks, S.; Zupancic, J. J.; Swedo, J. R. *Solid State Ionics* **1988**, *31*, 117.

(2) (a) Pickup, P. G.; Murray, R. W. *J. Electrochem. Soc.* **1984**, *131*, 833. (b) Pickup, P. G.; Kutner, W.; Leidner, C. R.; Murray, R. W. *J. Am. Chem. Soc.* **1984**, *106*, 1991. (c) Abruna, H. D.; Denisevich, P.; Umana, M.; Meyer, T. J.; Murray, R. W. *J. Am. Chem. Soc.* **1981**, *103*, 1. (d) Denisevich, P.; Wildman, K. W.; Murray, R. W. *J. Am. Chem. Soc.* **1981**, *103*, 4727.

(3) Kittlesen, G. P.; White, H. S.; Wrighton, M. S. *J. Am. Chem. Soc.* **1985**, *107*, 7373.

(4) (a) White, H. S.; Kittlesen, G. P.; Wrighton, M. S. *J. Am. Chem. Soc.* **1984**, *106*, 5375. (b) Kittlesen, G. P.; White, H. S.; Wrighton, M. S. *J. Am. Chem. Soc.* **1984**, *106*, 7389. (c) Natan, M. J.; Mallouk, T. E.; Wrighton, M. S. *J. Phys. Chem.* **1987**, *91*, 648. (d) Paul, E. W.; Ricco, A. J.; Wrighton, M. S. *J. Phys. Chem.* **1985**, *89*, 1441. (e) Wrighton, M. S.; Chao, S.; Chyan, O. M.; Jones, E. T. T.; Leventis, N.; Lofton, E. P.; Schloh, M. O.; Shu, C. F. *Chemically Modified Microelectrode Surfaces in Science and Industry*; Leyden, D. E.; Collins, W. T., Eds.; Gordon and Breach: New York, 1987; p 337. (f) Natan, M. J.; Wrighton, M. S. *Prog. Inorg. Chem.* **1989**, *37*, 391-494.

(5) Chao, S. C.; Wrighton, M. S. *J. Am. Chem. Soc.* **1987**, *109*, 2197.

(6) Chao, S. C.; Wrighton, M. S. *J. Am. Chem. Soc.* **1987**, *109*, 6627.

(7) Talham, D. R.; Crooks, R. M.; Cammarata, V.; Leventis, N.; Schloh, M. O.; Wrighton, M. S. *Lower-Dimensional System and Molecular Electronics*; Proceedings of NATO ASI, Spetses, Greece, 1990; Metzger, R. M., Day, P., Papavassiliou, G., Eds.; Plenum Press: New York, in press.

0897-4756/90/2802-0568$02.50/0

Scheme I. Cross-Sectional Views of "Solid-State" Microelectrochemical Devices: (A) WO_3-Based Transistor; (B) Polyaniline-Based Transistor; (C) WO_3 and Polyaniline Self-Referencing Transistor (See Text)

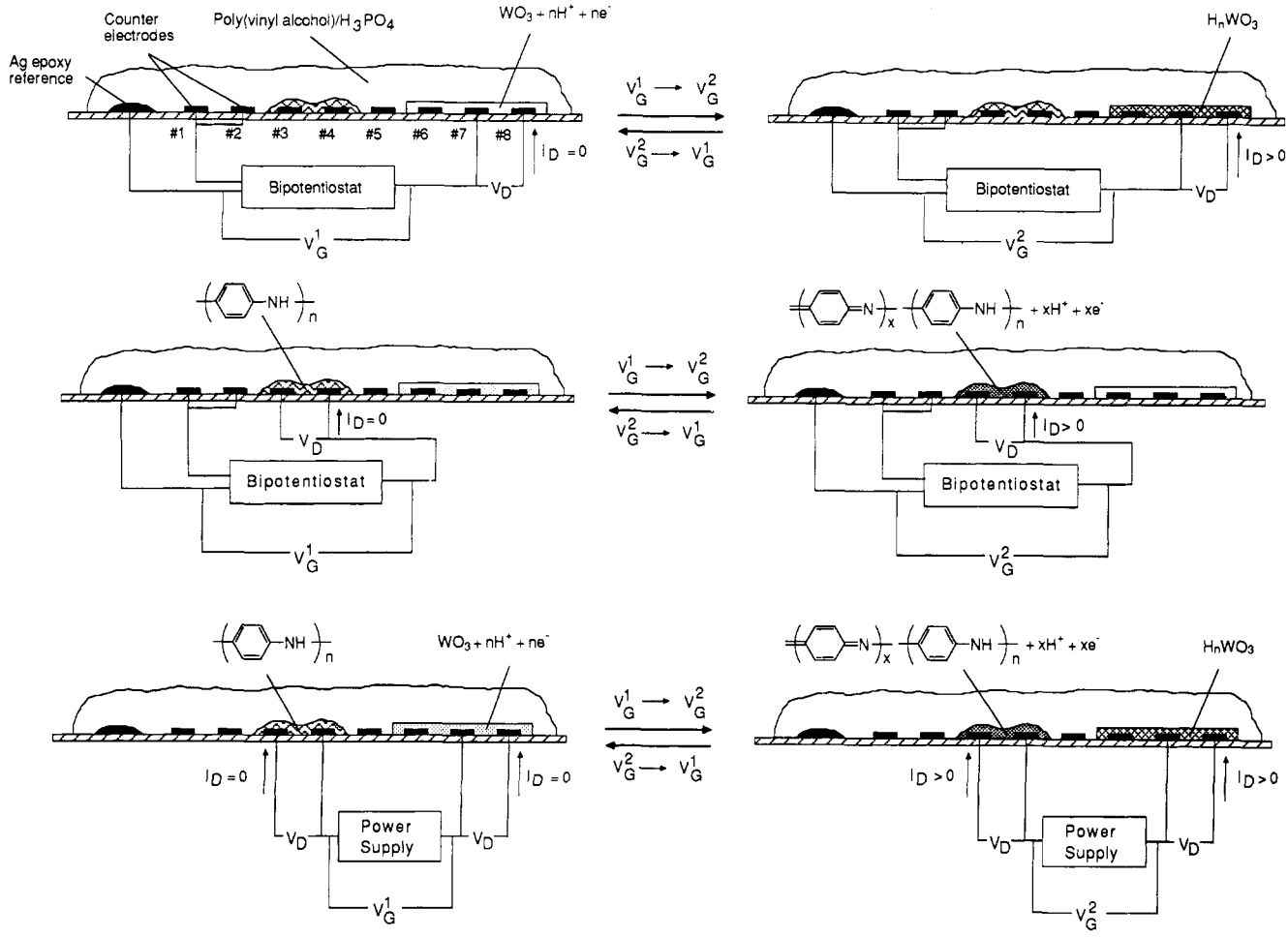

Scheme IA illustrates the methodology for the electrochemical characterization of WO_3 confined to electrodes 6–8. Basically, the relative conductivity as a function of electrochemical potential is determined by varying the gate potential, V_G, while monitoring the drain current, I_D, at a small fixed drain potential, V_D. Previous work has shown that reduction of WO_3 to H_nWO_3 in aqueous solution yields a highly conducting material.[4c] Polyaniline confined to microelectrodes 3 and 4, Scheme IB, can be characterized in an analogous way.[4d,6] The difference is that polyaniline is an insulator when reduced and becomes a conductor when oxidized.[4d,6] Thus, WO_3 and polyaniline have complementary behavior, suggesting the viability of the self-referencing transistors in Scheme IC where the application of a voltage in a two-terminal mode renders both materials conducting.

Polyaniline and WO_3 are also regarded as electrochemical energy-storage materials and can be used in combination as illustrated in Scheme IC to yield a surface storage device. The reversible charge and discharge shown in Scheme IC is strictly analogous to charge and discharge of a battery. This type of assembly of complementary redox materials on working and counterelectrode is commonly used in research on so-called electrochromic smart windows, which are of current interest for energy conservation in buildings and cars.[8]

For the system shown in Scheme IC, the self-referencing transistors, where the charge passed in changing V_G results in simultaneous switching of two transistors, it is important to recognize the need to have the proper ratio of polyaniline and WO_3 to achieve maximum conductivity in each material. To illustrate, if there is a very large amount of polyaniline and a small amount of WO_3, the WO_3 will be reduced completely and becomes conducting, while the polyaniline is only fractionally oxidized and will not be conducting. Establishing the relationships between potential, state of charge, and conductivity for both WO_3 and polyaniline is, therefore, critical to rational design of microelectrochemical systems.

Turning now to the combination of polyaniline and WO_3 to form microelectrochemical diodes, consider the remaining two systems described in this article, Scheme II. The electrical behavior of the WO_3/polyaniline junction in Scheme IIA may be understood in terms of the electrochemistry involved in both materials comprising the diode. For instance, if an electrical potential, V_{appl}, is applied across the WO_3/polyaniline junction such that the WO_3-derivatized microelectrode is biased positively with respect to the polyaniline-derivatized microelectrode (reverse bias), no current should pass through the junction, in part because WO_3 is insulating when oxidized and polyaniline is insulating when reduced. However, the key to rectification is that reduction of WO_3 by reduced polyaniline is not feasible thermodynamically. Upon forward bias (negative lead to WO_3), WO_3 can be reduced to a conducting tungsten bronze, H_nWO_3, and polyaniline is oxidized and also conducting. At the WO_3/polyaniline junction, charge is transported through the interface by the thermodynamically favored redox reaction between

(8) (a) Rauh, R. D.; Cogan, S. F. *Solid State Ionics* **1988**, *28–30*, 1707. (b) Nguyen, M. T.; Dao, L. H. *J. Electrochem. Soc.* **1989**, *7*, 2131.

Scheme II. Microelectrochemical Diode Based on WO_3 and Polyaniline: (A) WO_3 and Polyaniline in Direct Contact, Forming a WO_3/Polyaniline Junction; (B) WO_3 and Polyaniline Connected through an External Wire

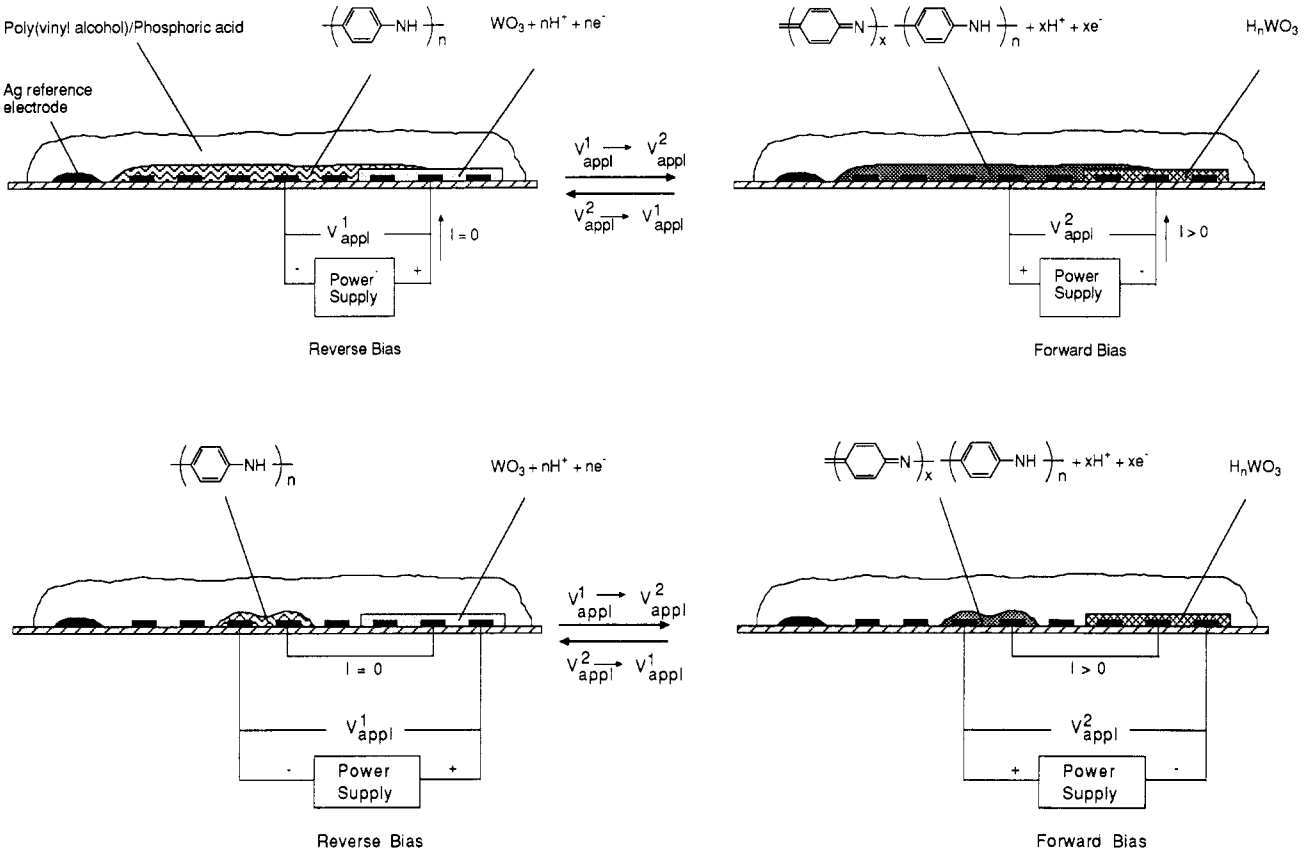

oxidized polyaniline and reduced H_nWO_3. The threshold voltage, V_T, of the WO_3/polyaniline-based solid-state microelectrochemical diode is approximately the difference in potential for oxidizing polyaniline and reducing WO_3. This difference is also the approximate switching potential for the self-referencing transistors, Scheme IC.

Importantly, we find that an actual junction between WO_3 and polyaniline is not required to demonstrate electrochemical rectification. A diodelike current–voltage characteristic can be obtained by simply externally connecting two separated WO_3-derivatized and polyaniline-derivatized microelectrodes with a wire, Scheme IIB. This contacting scheme has been introduced earlier by Murray and co-workers in their studies of redox bilayer materials.[2] The hardwire connection scheme greatly simplifies the assembly of microelectrochemical diodes, because a good electrical contact between diverse redox materials, e.g., conducting polymers and redox-active oxides, is not essential for rectification.

Experimental Section

Microelectrode Modification. The microfabrication process for derivatizing microelectrodes with WO_3 has previously been described.[9] The individual devices were mounted on TO-8 headers (Schott Electronics) with Ag–epoxy (Epoxy Technology) and encapsulated with clear epoxy (Hydrosol Division, Dexter Corp.). Subsequently, the WO_3-based device was cleaned in an O_2 plasma (100 mTorr, 200 W) for 4–5 min. The remaining microelectrodes were electrochemically cleaned by repeated potential excursions between −1.5 and −2.0 V vs a saturated calomel electrode (SCE) in 0.1 M K_2HPO_4. Polyaniline was selectively deposited on only two microelectrodes of the array by cycling the potential of the electrodes between −0.1 V to +0.85 V vs SCE in 0.1 M aniline (Aldrich)/0.5 M $NaHSO_4$/0.6 M H_2SO_4 solution, while all remaining electrodes were kept at −0.1 V vs SCE. To make devices with a WO_3/polyaniline connection, all electrodes were scanned between −0.1 V and +0.85 V vs SCE, except the WO_3-derivatized electrodes, which were not under potential control. For the independent characterization of the two redox materials confined to the microelectrodes of the solid-state device, two bare Pt microelectrodes were used as the counterelectrodes and a small spot of Ag epoxy (close to the microelectrode array area) served as a quasi-reference electrode. The whole device active area was then covered with a drop of an aqueous solution containing 0.2 mM poly(vinyl alcohol) (Polysciences), MW = 1.33×10^5, 99% hydrolyzed, and 0.15 M H_3PO_4. The solid-state device is completed by evaporation of the H_2O at 35 °C for 24 h. The resulting transparent film contains one H_3PO_4 per four poly(vinyl alcohol) repeat units. To estimate the typical thickness resulting from one drop of aqueous poly(vinyl alcohol)/H_3PO_4 solution, we placed a drop on a microscope slide, dried it, and determined its thickness by surface profilometry to be ~20 μm.

Ac Impedance Analysis. A Solartron 1255 HF frequency response analyzer combined with a Solartron 1286 electrochemical interface was used for impedance measurements. The ac excitation was 20 mV, and spectra were taken in the frequency range between 1 Hz and 100 kHz. A simple impedance cell was constructed by scratching a narrow groove through a thin (0.1 μm) Pt layer evaporated onto a glass slide. The electrolyte solution was then cast on top of the two-electrode open-sandwich impedance cell and dried at room temperature. The open-face arrangement of the two ~1-cm^2 electrodes was used to facilitate the rapid hydration and dehydration of the electrolyte film. The geometry is thus not ideal for absolute measurement but gives excellent relative resistances. Ac impedance measurements using clean microelectrode arrays were attempted, but apparently the impedance change in the solid electrolyte is obscured by the considerable impedance of the microelectrode array and connection leads. Regular gas wash bottles were used to repeatedly hydrate and dry the Ar gas or air that was blown over the im-

(9) Schloh, M. O.; Leventis, N.; Wrighton, M. S. *J. Appl. Phys.* **1989**, *66*, 965.

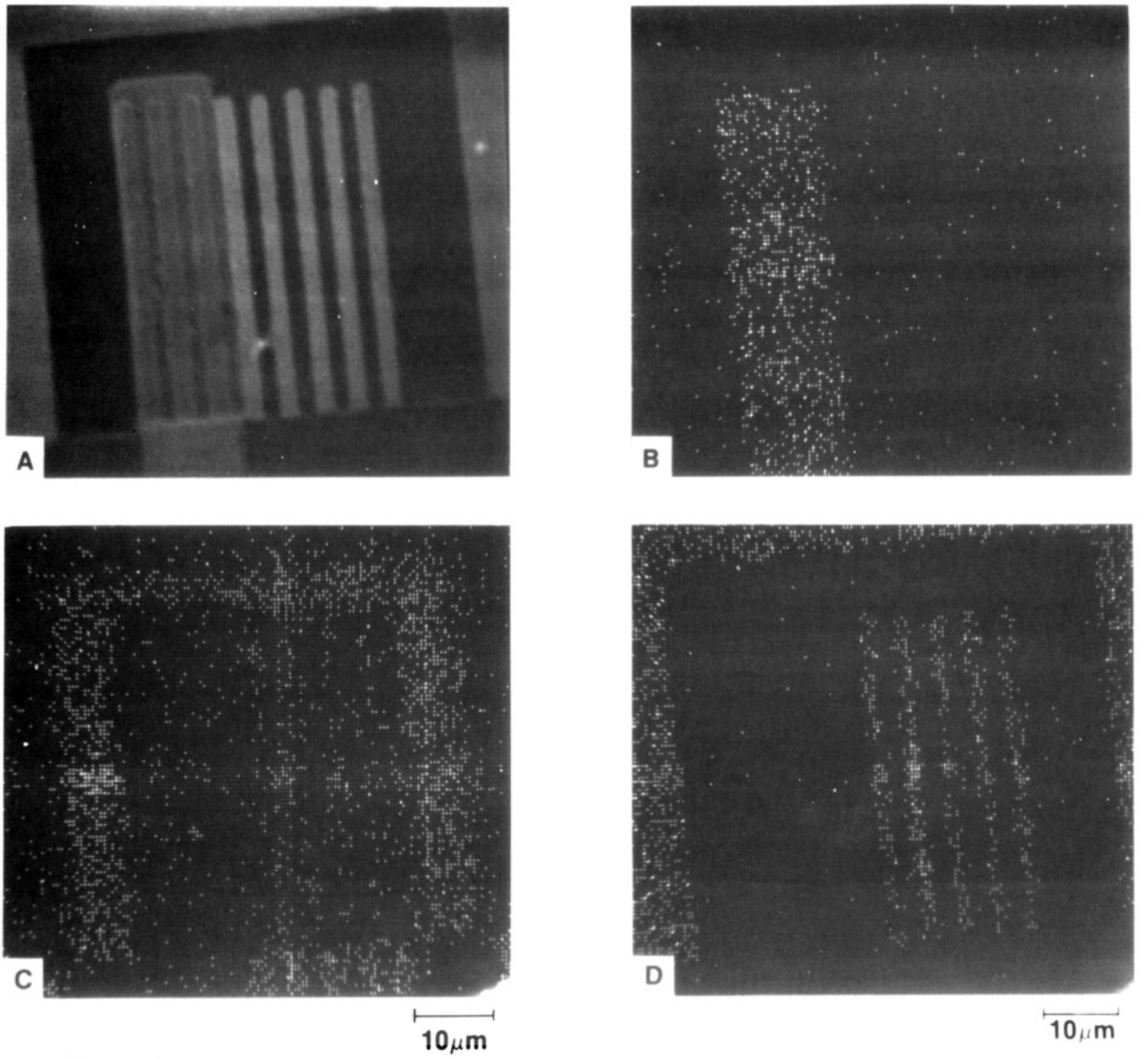

Figure 1. Element distribution as seen by the scanning Auger microprobe: (A) SEM picture obtained with the electron microprobe of the Auger spectrometer at 1500X magnification; (B) tungsten map; (C) silicon map; (D) platinum map.

pedance cell. The impedance cell was housed in a glass flask.

Auger Surface Analysis. The analysis by scanning Auger spectroscopy of a conducting material on an insulator has previously been complicated by differential charging. This problem was overcome by carefully placing a thin coating of silver paint on the insulating layer around the array and grounding the electrodes at the same time. The paint was dried for ~5 min in air and then in an oven at 90 °C for 15 min. Finally the sample was grounded with Ag paint to a piece of Cu tape which, in turn, was grounded to the spectrometer.

Auger spectra were obtained with a PDP 11/04-controlled Physical Electronics (Perkin Elmer) Model 590 scanning Auger microprobe spectrometer (SAM) employing a 0.8-μm, 80–100-nA, 10-keV electron beam for excitation and a cylindrical mirror analyzer (CMA) for detection. For mapping, the electron beam energies were chosen to maximize the peak-to-peak amplitude of the Auger spectra plotted in the derivative mode. The difference between the magnitudes of the peak-to-peak separation corresponded to signal intensity. The signals were segregated into three levels of varying intensity and displayed on a 160 × 160 array. Surface sputtering of the sample prior to analysis to remove carbon-containing impurities was accomplished using a 2-keV, 5.0 nA/cm^2 Ar^+ beam.

Electrochemical Equipment. Electrochemical experiments were carried out with use of a Pine Instruments Model RDE-4 bipotentiostat. Voltammetric traces were recorded on a Kipp and Zonen Model BD 91 *XYY'* recorder with the zero suppression option and a time base function. A Nicolet Model 4094B digital oscilloscope with Model 4570 digitizer and Model F-43 disk drive plug-ins was used for the high-frequency characterization experiments. For the potential variation we used either the linear output of a PAR Model 175 programmer or the sinusoidal waveform of the internal oscillator output of a PAR Model 5204 lock-in amplifier.

Results and Discussion

Surface Characterization by Auger Spectroscopy. With a combination of photolithographic and dry etching processes a thin film of polycrystalline WO_3 can be patterned to selectively cover a fraction of eight individually addressable and closely spaced (~1.2 μm apart) Pt microelectrodes (~50 μm long, 2.5 μm wide, and 0.1 μm thick).[9] The modified microelectrode array can be characterized by Auger electron spectroscopy, which provides surface elemental analysis of the surface, to establish the success of the microfabrication process.

Figure 1A shows a low-resolution SEM micrograph indicating the region of a chip covered by WO_3. Figure 2 shows three Auger electron spectra taken on different areas of such a WO_3-coated chip. The spectra are shown for the

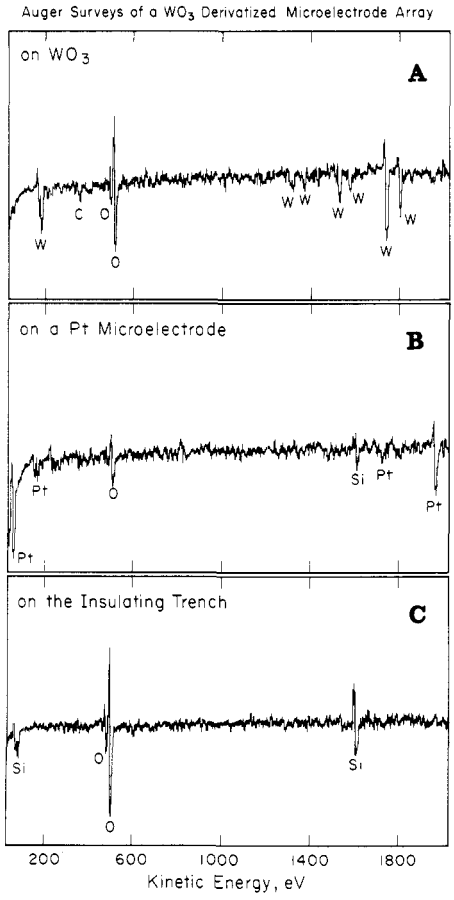

Figure 2. Scanning Auger microprobe surveys: (A) on WO_3; (B) on an underivatized Pt microelectrode; (C) on the trench between the array and the Pt protective barrier.

WO_3-coated region (Figure 2A), for a bare Pt microelectrode (Figure 2B), and for the insulating trench around the microelectrodes (Figure 2C). The important information from these spectra is that (1) only W and O are present in the area where WO_3 is claimed to be confined and (2) the Pt electrodes show no evidence of W. The Pt electrodes show Pt, Si, and O in the survey, Figure 2B, but the Si and O are due to the fact that the beam size has a slightly larger diameter than the width of the microelectrodes, so that Si and O from the substrate are also detected.

A collection of Auger element maps obtained for a WO_3-coated chip is included in Figure 1. The maps represent the distribution of elements over the surface of the chips. To map W, the primary peak at 1736 eV was used. Due to overlapping Auger electron emission energies it was necessary to use the third most intense peak for Pt, at 1967 eV, and the second most intense peak for Si at 1619 eV. The W and Pt images are virtually noise-free and look very clean, Figure 1B,D. However, the use of the secondary peak for Si gave a noisy image, Figure 1C, owing to a poor signal-to-noise ratio. Overall, both the Auger survey spectra and the Auger element maps clearly indicate that WO_3 has been confined to three microelectrodes of the array. Equally important in our present work is the fact that the remaining five microelectrodes are free of WO_3 and are available for further derivatization with polyaniline by polymerization of aniline.

Characterization of Poly(vinyl alcohol)/H_3PO_4 Solid-State Electrolyte. Poly(vinyl alcohol)/H_3PO_4 mixtures have recently attracted interest due to their high ionic conductivity at room temperature when dried to a film.[1] The mixtures are prepared by dissolving poly(vinyl

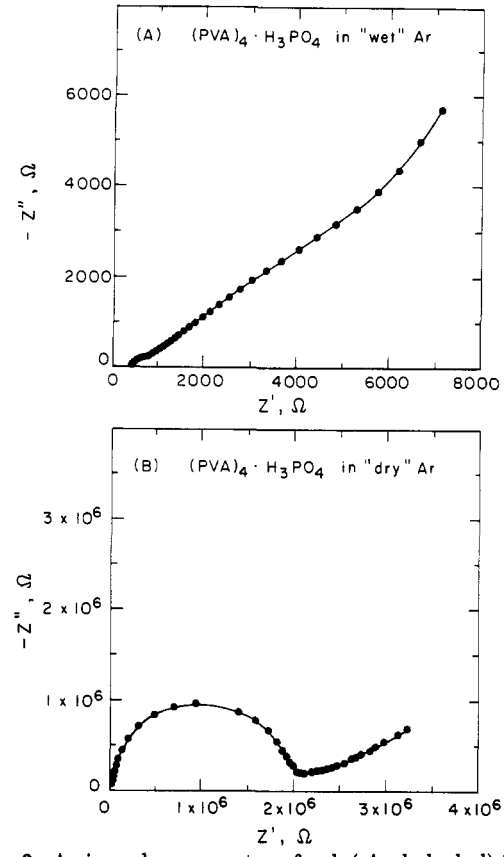

Figure 3. Ac impedance spectra of poly(vinyl alcohol)/H_3PO_4 film in (A) hydrated "wet" Ar atmosphere and (B) dry Ar atmosphere. The highest frequency used is 100 kHz (extreme left point) and the low frequency is 1 Hz (extreme right point). The ionic resistance of the dry polymeric electrolyte is $R = 2.2 \times 10^6$ Ω for the impedance cell used. The resistance of the polymeric electrolyte drops to $R = 800$ Ω in the hydrated state.

alcohol) and H_3PO_4 in a ratio of 4:1 polymer repeat units per acid molecule in hot H_2O.[1] When this mixture is dried, a solvent-swollen solid polymeric electrolyte film is obtained whose conductivity depends on the amount of H_2O in the poly(vinyl alcohol)/H_3PO_4 film.

We have used standard ac impedance techniques[10] to determine the extent of change of ionic conductivity in the electrolyte film upon variation of the atmosphere from H_2O-free to H_2O-saturated. Figure 3 shows the ac impedance spectrum for a "dry" poly(vinyl alcohol)/H_3PO_4 film. This spectrum features a large semicircle and a spur. This response agrees with the data reported by Petty-Weeks and Polak[1b] and is often encountered for solid electrolytes.[10] The intersect of the low-frequency end of the semicircle with the real axis yields the ionic resistance R of the electrolyte for this particular impedance cell. The specific resistivity, ρ, can be calculated if the separation of the electrodes, l, and the electrode area, A, is known: $\rho = (RA/l$. We can only estimate the actual A/l, owing to the open-face electrode structure, but our dry-state specific resistivities are in reasonable accord with data of Polak.[1b] The ionic resistance of a "dry" film is $\sim 2.2 \times 10^6$ Ω or $\rho = 4.4 \times 10^6$ Ω cm. When the gas flow is switched to H_2O-saturated Ar gas (or H_2O-saturated air), the ac impedance spectrum, Figure 3, exhibits only a poorly developed semicircle. The resistance of the electrolyte in its "wet" state is significantly lower than the "dry" state, on

(10) (a) Bruce, P. G. *Polymer Electrolyte Reviews—1*; MacCallum, J. R., Vincent, C. A., Eds.; Elsevier Applied Science: London, 1987; p 237. (b) Ratner, M. A.; Shriver, D. F. *Chem. Rev.* **1988**, *88*, 109.

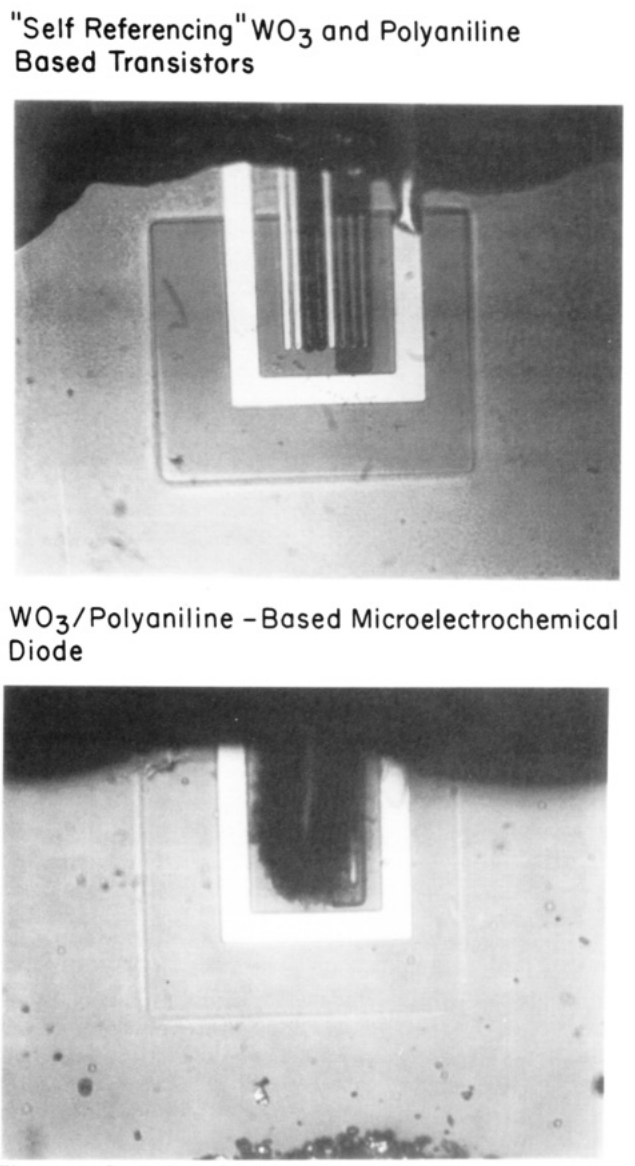

Figure 4. Optical micrographs of (top) a "self-referencing" WO_3 and polyaniline device, where WO_3 and polyaniline are not in contact with each other, and (bottom) a WO_3/polyaniline diode with a physical connection between the two materials.

the order of 800 Ω or $\rho = 1.6 \times 10^3$ Ω cm. The presence of a separate phosphoric acid/water phase, which is responsible for the H^+ conduction in the H_2O swollen polymer film, has been reported.[1b] The important point is that the conductivity of the poly(vinyl alcohol)/H_3PO_4 film can be reversibly and rapidly (~30 s) modulated by changing the H_2O content of the ambient gas. Since the dry film is a high-resistance ionic conductor, reduction of WO_3 or oxidation of polyaniline in this medium will be sluggish in comparison to that in the hydrated film. Accordingly, our characterizations of the five electrochemical systems shown in Schemes I and II have been generally carried out in H_2O-saturated gases.

Electrochemical Characterization of WO_3 and Polyaniline in Poly(vinyl alcohol)/H_3PO_3 Solid Electrolyte. Optical micrographs of two modified microelectrode arrays are shown in Figure 4. The device in the upper half of the figure consists of three WO_3-coated microelectrodes adjacent to one bare microelectrode, next to which are two polyaniline-coated microelectrodes. A Ag spot (out of the field of view) is used as the quasi-reference electrode, and the two remaining microelectrodes on the left side of the microelectrode array are shorted

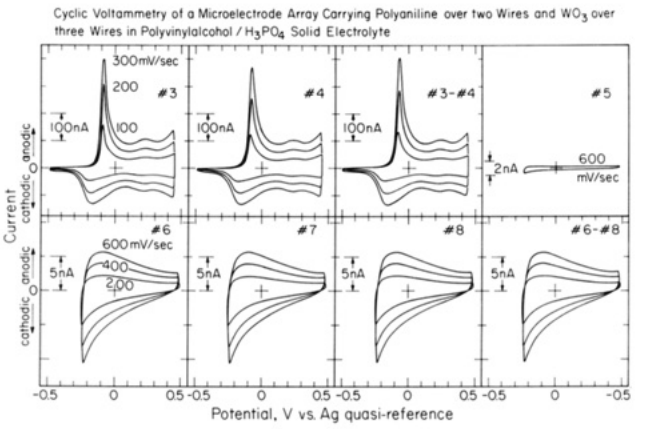

Figure 5. Cyclic voltammetry of polyaniline and WO_3 confined on an eight microelectrode array vs a Ag quasi-reference electrode. The device is covered by a thin film of poly(vinyl alcohol)/H_3PO_4 solid electrolyte and kept in a H_2O-saturated Ar atmosphere.

together and used as the counterelectrode. The chip shown in the upper half of Figure 4 can be used to characterize all systems shown in Scheme I and the hardwired diode shown in Scheme IIB. In the lower half of Figure 4, polyaniline has been grown on all five, previously, bare, microelectrodes and overcoats the WO_3-coated microelectrodes. This array can be used to characterize the system in Scheme IIA.

Cyclic voltammetric characterization of the array depicted in the top half of Figure 4 is shown in Figure 5. Microelectrodes 3 and 4 exhibit electrochemistry typical of polyaniline.[4d,6] The fact that the shape of the cyclic voltammogram for electrodes 3 and 4 scanned separately is the same as when both electrodes are scanned together at all scan rates indicates that polyaniline electrically connects the two electrodes. The electrochemical response of WO_3-coated microelectrodes 6–8 the array is similar to the electrochemistry observed for WO_3 in aqueous acid electrolyte, and we conclude that reduction of WO_3 to H_nWO_3 occurs in the solid H^+ conductor.[4c] Examination of the polyaniline and WO_3 upon oxidation and reduction by optical microscopy shows the green coloration expected for oxidized polyaniline and the blue coloration for reduced WO_3.

Solid-State Microelectrochemical Transistors Based on WO_3 and Polyaniline. The ability to reversibly reduce WO_3 suggests the possibility of a WO_3-based solid-state transistor as previously demonstrated for polyaniline.[6] As for polyaniline-coated microelectrodes, H_2O-dependent electrochemical behavior is also observed for WO_3 under a poly(vinyl alcohol)/H_3PO_4 solid electrolyte film. Microelectrochemical transistors based on WO_3-functionalized microelectrodes work on the principle that the conductivity of the redox material is a function of the state of charge (cf. Scheme IA). For the case of a WO_3-based device, the oxidized form of WO_3 is an insulator, and the reduced, proton-intercalated form, H_nWO_3, is an electronic conductor. Therefore, as the gate potential, V_G^1, which controls the state of charge, is moved from an oxidizing potential to a reducing potential, V_G^2, a drain current, I_D, will flow between the microelectrodes (7 and 8 in Scheme IA) for a fixed drain potential, V_D. Figure 6 includes a typical plot of drain current, I_D, vs gate voltage, V_G. The switching characteristics of WO_3 in hydrated poly(vinyl alcohol)/H_3PO_4 are essentially the same as the electrochemical response found in aqueous acidic electrolytes.[4c,9] By switching the atmosphere surrounding the WO_3-based device from H_2O-saturated Ar to dry Ar, the device cannot be "switched-on" by sweeping to a

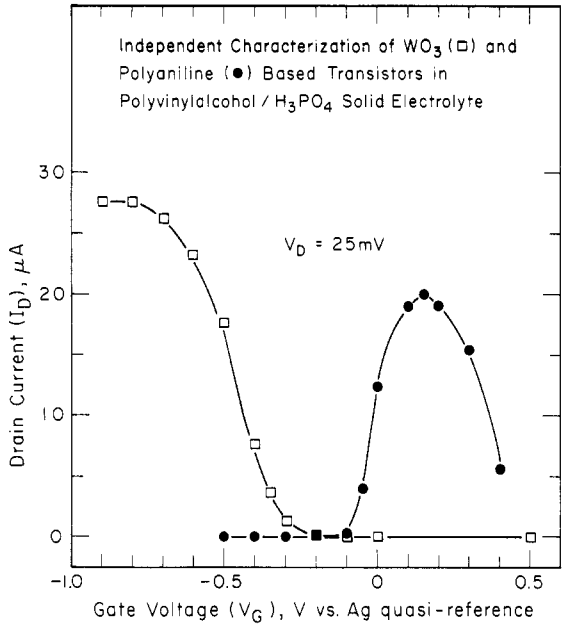

Figure 6. Switching characteristics of WO_3 and polyaniline on the same chip addressed independently. These characteristics are for devices shown in Schemes IA and IB.

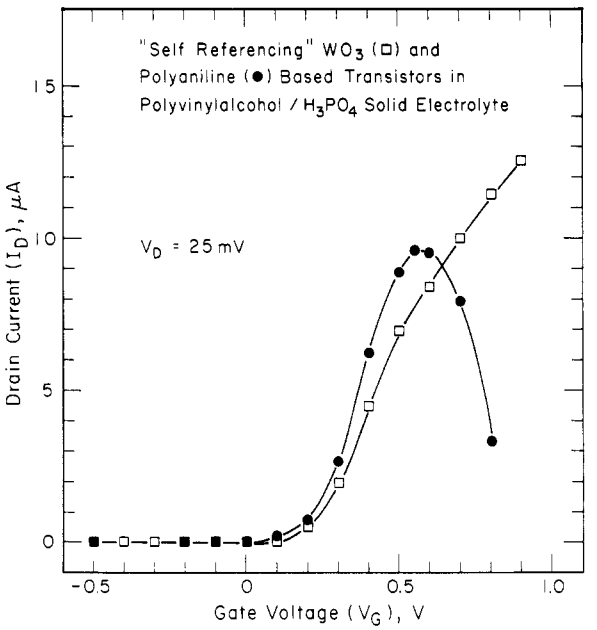

Figure 7. Switching characteristics of WO_3 and polyaniline on the same chip referenced one vs the other. These characteristics are for the device shown in Scheme IC.

negative potential and WO_3 remains an insulator until H_2O is introduced into the Ar atmosphere. This is an expected result in view of the fact that the mobility of the intercalating species, H^+, is impeded in the dry, solid-state electrolyte. Hence reduction of WO_3 to H_nWO_3 cannot be effected. Along the same line of reasoning, when the WO_3 device is already in its "switched-on" or conducting state, H_nWO_3, and the atmosphere surrounding the device is changed from H_2O-saturated to dry gas, the device stays in the conducting form even when V_G is moved to a potential where H_nWO_3 should be oxidized to WO_3.

Figure 6 confirms that polyaniline- and WO_3-based transistors on the same chip, Figure 4, addressed independently yield characteristics identical with those obtained when the polyaniline or WO_3 are on different chips. Thus, the fabrication processes yield a chip that has two microelectrochemical transistors. WO_3 is "switched on" at some negative potential, V_G, depending on the availability of protons, and its conductivity reaches a plateau as the material is driven to more a negative V_G. Polyaniline, on the other hand, becomes conducting at positive V_G, and its conductivity reaches a maximum value at +0.45 V vs Ag quasi-reference.[6] The independent characterization of WO_3 and polyaniline against a common reference electrode, i.e., the Ag quasi-reference, clearly shows that there is a region of gate potential, about 200 mV wide, in which neither material is appreciably conducting.

The simultaneous switching of both the polyaniline- and WO_3-based transistors is possible if one redox material is used as the reference for the other, Scheme IC. The potential at which both materials become conducting or the turn-on potential, V_T, should be about 200 mV as predicted by the difference in V_G, where polyaniline and WO_3 become conducting, Figure 6. The value of V_T from the self-referencing transistor is thus characteristic of the two switching materials employed in the system. However, the simultaneous switching of the two materials also depends on balancing the amounts present such that the electrons removed from polyaniline to result in a conductor will be adequate to effect sufficient reduction of WO_3 to render it conducting. Integration of cyclic voltammograms like those in Figure 5 and comparison of the potential limits with the I_D–V_G plots for the individual transistors in Figure 6 can be used to gauge whether the materials are adequately balanced. In our experiments we are typically dealing with $\sim 10^{-7}$ C in order to effect switching of either the WO_3- or polyaniline-based transistors. Figure 8 shows that a single applied potential can be used to effect simultaneous switching of the WO_3- and polyaniline-based transistors on the same chip. In this system a small drain potential, V_D, applied across a pair of microelectrodes coated with WO_3 or polyaniline (cf. Scheme IC) allows simultaneous monitoring of the conductivity of each material as a function of V_G. As illustrated in Figure 7, I_D in *both* transistors becomes significant for $V_G > 200$ mV, as expected.

Characterization of Rectifying Devices by Interfacing Polyaniline with WO_3. The optical micrograph in Figure 4, bottom, shows a microelectrochemical system where polyaniline has been grown over some large fraction of the WO_3-coated microelectrodes, ensuring intimate contact between the two redox materials. The electrical characterization of a two-terminal device based on this junction, Scheme IIA, shows that large current densities, on the order of 1 A/cm^2, can be driven across the junction in only one direction. The turn-on potential is about 200 mV, consistent with results from the independent characterization of the two materials and the self-referencing device.

The rectification behavior observed may be understood in terms of the electrochemistry involved in each of the two materials comprising the diode junction. The key to the diodelike current–potential curve is that oxidized polyaniline can oxidize the H_nWO_3, but reduced polyaniline cannot reduce WO_3 owing to the difference in their redox potentials. Thus, the redox process occurring at the WO_3/polyaniline interface is sufficiently thermodynamically downhill in only one direction that charge transport across the interface is effectively unidirectional.

To achieve a microelectrochemical diode, WO_3 and polyaniline do not have to be in physical contact, Scheme IIB. In Figure 8 the two-terminal current–voltage characteristic of a microelectrochemical device is shown where WO_3 and polyaniline are not in physical contact with each other. As

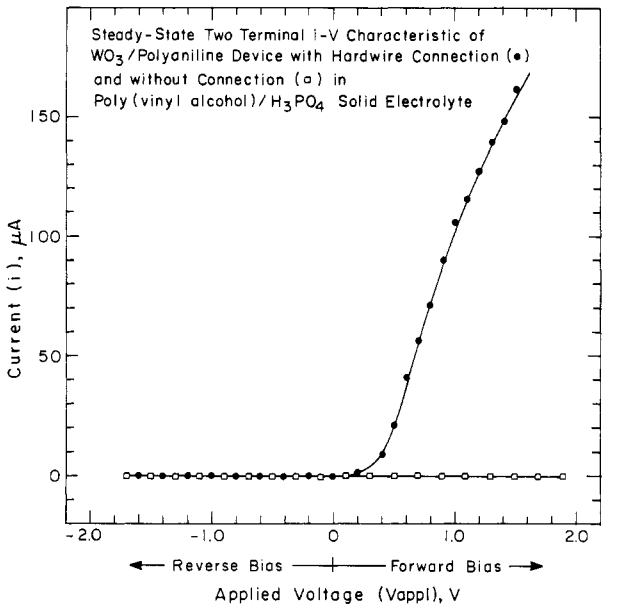

Figure 8. Steady-state two terminal current–voltage characteristic of a WO_3/polyaniline device (●) with hardwire connection between the redox materials and (○) without hardwire connection. These characteristics are for the device shown in Scheme IIB.

expected, no steady-state current passes through the two-terminal device when the circuit between WO_3 and polyaniline is not completed. However, a simple external hardwire connection as schematically represented in Scheme IIB restores a complete electrical circuit, and rectifying behavior is found.

An important difference between the diode device in Figure 8 and the transistors (Figures 6 and 7) is the rather large currents observed at forward bias for the diode compared to the modest currents observed during I_D vs V_G characterizations of the transistors. The diode currents for diodes having a direct WO_3/polyaniline contact are even larger than the diode shown in Figure 8. For the diodes the bias across the junction is much larger (1–2 V) compared to the small value (25 mV) of V_D applied across two microelectrodes in the transistors. Second, the limiting thickness of the WO_3 layer for the diode with a direct WO_3/polyaniline contact is not 1.2 μm, i.e., spacing between microelectrodes, but ~0.3 μm, which is the thickness of the layer of WO_3 over which the polyaniline is grown. In the case of the hardwire connection diode, Figure 8, the observed current through the device is somewhat lower than that for the case of a physical connection between WO_3 and polyaniline because the circuit is completed through a longer current path involving two polyaniline-covered and two WO_3-covered microelectrodes both spaced ~1.2 μm apart, thus adding a resistive element to the circuit.

Interestingly, the diode devices like that shown in Figure 4, bottom, can be evaluated with and without a hardwire connection in parallel with the physical contact between the WO_3 and polyaniline. The hardwire contact is obviously independent of the kinetics for charge transport across the physical contact between the two materials. If the charge transport across the physical contact limited the diode current, the hardwire connection would result in a larger diode current under forward bias. We find no effect on the diode current in such a test and conclude that the diode current is limited by the charge-transport properties of the bulk materials. From the data in Figures 6 and 7 the H_nWO_3 and oxidized polyaniline show similar maximum conductivity. Thus, the diode currents are more

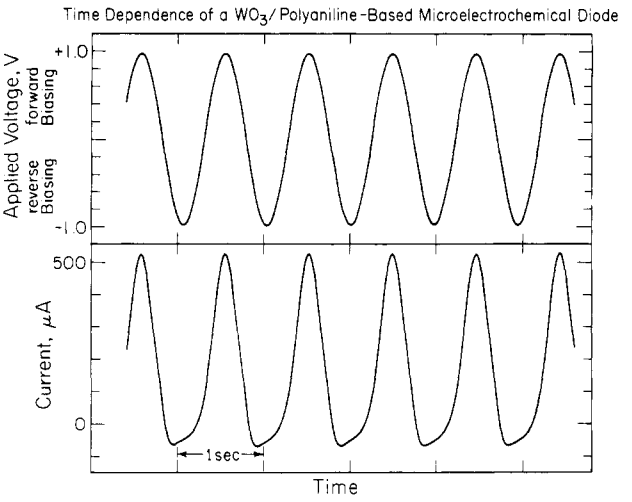

Figure 9. Plot of the current, I, and applied potential, V, vs time at 1-Hz frequency for a WO_3/polyaniline-based diode operated at 298 K in poly(vinyl alcohol)/H_3PO_4 solid electrolyte. The variation in V is from −1.0 V ($I = 0$) to +1.0 V ($I > 0$). $I_{forward}/I_{reverse} = 8.8$. The data here are for a device like that shown in Scheme IIB; cf also Table I.

Table I. Rectification Factors of the WO_3/Polyaniline-Based Diodes in Poly(vinyl alcohol)/H_3PO_4 Solid Electrolyte as a Function of Frequency[a]

freq,[b] Hz	I_f, μA	I_r, μA	I_f/I_r
steady state	640	1.5	427
0.0125 (l)	705	14	14.9
0.025 (l)	570	45	12.7
0.125 (l)	560	55	10.2
0.50 (l)	520	55	9.5
1.0 (s)	525	60	8.8
1.25 (l)	465	55	8.5
5 (s)	135	45	3.0
10 (s)	135	55	2.5
100 (s)	145	95	1.5
1000 (s)	70	50	1.4

[a] I_f and I_r correspond to +1.0 and −1.0 V biasing, respectively. [b] l, linear sweep; s, sinusoidal sweep.

or less equally dependent on the WO_3 and polyaniline.

The maximum forward bias of the diodes is about +2.0 V, because the devices decay quickly at +2.3 to +2.4 V forward bias, as can be concluded from an irreversible decline of forward current. When the diodes are reverse-biased, only a small current is observed, on the order of 1–10 μA at 1.0 V in Figure 8. A reverse bias breakdown occurs at about 2.0 V. Devices remaining at that voltage for long times also tend to lose their ability to "switch on" under forward bias. Examination by optical microscopy reveals that upon breakdown, either under forward or reverse bias, the polyaniline films have pealed off the microelectrodes and gas bubbles, presumably H_2 or O_2, are trapped in the solid electrolyte just above the array.

The current–voltage characteristic shown in Figure 8 is a steady-state curve in the sense that each data point is obtained after several minutes, typically 5 min, in order to allow the device to equilibrate under the new bias. If an alternating potential between the extremes of +1.0 V and −1.0 V is fed into the two-terminal device and the current is recorded, the rectification factors with respect to frequency can be determined. In Figure 9, the results of such an experiment are shown for a diode with the physical contact between the WO_3 and polyaniline. A sinusoidal potential variation with 1-Hz frequency is illustrated. Defining the ratio $I_{forward}/I_{reverse}$ as the rectification factor of the device at a given frequency, a measure

of the response time can be gathered, Table I. The main point is that the current response of the WO_3/polyaniline junction is sluggish. Even at only 1 Hz, $I_{forward}/I_{reverse}$ = 8.8, which is already about 50 times lower than the steady-state rectification factor, indicating a fairly large delay in the discharge of the two materials. Interestingly, even at 1 kHz the devices retain some rectification ability, as is demonstrated by the value of the rectification factor, which is still slightly larger than unity (~1.4). While polyaniline switches rapidly between its insulating and conducting states, up to 1 kHz in liquid electrolyte[11] and up to 100 Hz in poly(vinyl alcohol)/H_3PO_4 solid electrolyte,[4] the kinetics of WO_3 redox chemistry are found to be more sluggish. Switching speeds on the order of only several hertz even in aqueous acid[4c] have been reported. Therefore, we attribute the sluggish switching of the diode device to the slow response of WO_3 and not to the slow response of polyaniline.

Conclusion

Both WO_3 and polyaniline have been confined in a controlled manner onto a microelectrode array consisting of eight individually addressable microelectrodes. Both the amount and spatial distribution of the redox materials can be controlled to yield various electrochemical systems yielding characteristics that stem from the properties of the individual components. The redox materials can be placed either separately (to yield transistors or diodes) or in physical contact (to yield diodes) on the microelectrode array. The poly(vinyl alcohol)/H_3PO_4 solid-state polymer electrolyte is used to cover the assembly of derivatized microelectrodes. The switching properties of the resulting "solid-state" devices have been characterized, and a microelectrochemical, solid-state rectifying device based on the interface of WO_3 with polyaniline has been assembled. Interestingly, the two redox materials do not have to be in physical contact as long as there is a hardwire connection between them. The hardwire connection procedure may be useful in constructing a myriad of diode devices based on redox materials with widely different properties where a good, direct connection between the materials may be difficult to achieve. Additionally, the hardwire approach allows a chip to be reconfigured *after* being derivatized with different redox materials. For example, an array of eight microelectrodes could be functionalized with four redox materials to give four individually addressable transistors or be hardwired to give six different diodes. Obviously, the reconfiguration of diodes having physical junctions would be difficult. However, the maximum number of independently operating diodes on the eight electrode array with hardwire connections is two requiring three redox materials, whereas physical junctions would allow as many as four independently operating diodes using four different materials.

Acknowledgment. We thank Professor D. R. Sadoway for the use of his impedance equipment. We thank the Office of Naval Research and the Defense Advanced Research Projects Agency (University Research Initiative) for partial financial support.

Registry No. Pt, 7440-06-4; Au, 7440-57-5; WO_3, 1314-35-8; H_3PO_4, 7664-38-2; H^+, 12408-02-5; H_2SO_4, 7664-93-9; $NaHSO_4$, 7681-38-1; H_2O, 7732-18-5; polyaniline, 25233-30-1; poly(vinyl alcohol), 9002-89-5; aniline, 62-53-3.

(11) Lofton, E. P.; Thackeray, J. W.; Wrighton, M. S. *J. Phys. Chem.* **1986**, *90*, 6080.

Diffusion of Cesium Ion in SiO_2 Films Derived from Sol-Gel Precursors[1]

Carol L. Schutte[†,‡] and George M. Whitesides*[,†]

Department of Chemistry, Harvard University, Cambridge, Massachusetts 02138, and Department of Materials Science and Engineering, Massachusetts Institute of Technology, Cambridge, Massachusetts 02139

Received March 3, 1990

Hydrolyzed tetraethylorthosilicate (TEOS) formed SiO_2 gel films after being spin-coated onto silicon substrates and heated to temperatures ranging between 200 and 800 °C to effect different degrees of transformation from gel to glass. The index of refraction of the films increased from 1.42 at 25 °C to 1.45 after thermal treatment at 800 °C; the thickness of the films decreased by 29 ± 6%. These thermally pretreated gels were coated with a second film of sol-gel-derived SiO_2 doped with cesium chloride. Diffusion of the cesium ion through the undoped SiO_2 gels was studied by measurement of the depth profile of cesium by Rutherford backscattering spectroscopy. Increasing the temperature to which the undoped layer had been exposed decreased the extent of its infiltration or diffusion by cesium at room temperature. Diffusion of cesium at high temperature (≥750 °C) was, however, independent of the thermal history of the undoped layer, indicating that the rate at which the silica film transforms from gel to glass is faster than that at which cesium diffuses.

Introduction

The mobility of dopants in SiO_2 films made from sol-gel precursors—suspensions of silicate particles produced by polymerization involving hydrolysis and condensation reactions of silicon alkoxides[2]—is important in applications of these films.[3-9] Studies of diffusion in sol-gel systems have focused on diffusion of liquids into porous gels;[10]

† Harvard University.
‡ Massachusetts Institute of Technology.

(1) Supported in part by the National Science Foundation (CHE-88-12709) and the Defense Advanced Research Projects Agency through the University Research Initiative. The Cambridge Accelerator for Materials Science was purchased and supported (in part) through a DARPA/URI grant and is housed in the Harvard University Materials Science Research Laboratory, an NSF-funded facility (DMR-86-14003).

0897-4756/90/2802-0576$02.50/0